Isosorbide-2-carbamate Esters: Potent and Selective Butyrylcholinesterase Inhibitors

Ciaran G. Carolan,[†] Gerald P. Dillon,[†] Joanne M. Gaynor,[‡] Sean Reidy,[‡] Sheila A. Ryder,[†] Denise Khan,[†] Juan F. Marquez,[†] and John F. Gilmer*[,†]

School of Pharmacy and Pharmaceutical Sciences, Trinity College, Dublin 2, Ireland

Received May 14, 2008

In this study, we report the SAR and characterization of two groups of isosorbide-based cholinesterase inhibitors. The first was based directly on the clinically used nitrate isosorbide mononitrate (ISMN) retention of the 5-nitrate group and introduction of a series of 2-carbamate functionalities. The compounds proved to be potent and selective inhibitors of human plasma butyrylcholinesterase (*hu*BuChE). In the second group, the nitrate ester was removed and replaced with a variety of alkyl and aryl esters. These generally exhibited nanomolar potency with high selectivity for BuChE over acetylcholinesterase (AChE). The most potent and selective compound was isosorbide-2-benzyl carbamate-5-benzoate with an IC_{50} of 4.3 nM for BuChE and >50000 fold selectivity over human erythrocyte AChE. Inhibition with these compounds is time-dependent, competitive, and slowly reversible, indicating active site carbamylation.

Introduction

There are two types of cholinesterase enzymes found in vertebrates: acetylcholinesterase (EC 3.1.1.7; AChE[a]) and butyrylcholinesterase (EC 3.1.1.8; BuChE). These are probably the most widely studied enzymes due to their extraordinary efficiency and the classical relationship between AChE and the neurotransmitter acetylcholine. AChE has been a drug target for the treatment of Alzheimer's disease (AD) since the emergence of the cholinergic hypothesis of AD over 25 years ago. This followed recognition that the cognitive impairments in AD correlated with cholinergic deficits such as reduced synaptic acetylcholine synthesis and choline acetyltransferase (ChAT) activity.[1,2] These observations were made just as the role of the cholinergic system in memory processing and learning began to be more widely appreciated.[3] The introduction of the cholinesterase inhibitors (CHIs), first tacrine then donepezil, rivastigmine, and galantamine, has made an important contribution to the management and well-being of early stage AD patients, although significant scientific and clinical questions about these remain.

In the past few years, CHI medicinal chemistry has diversified from pure AChE inhibitor design into a number of related strategies: (i) dual binding site inhibitors that bind at the active site *and* at the AChE peripheral site, which catalyzes the aggregation of β-amyloid in vitro[4,5] (dual binding site occupancy has also led to the compounds of femtomolar potency[6]); (ii) hybrid compounds that affect both the metabolism of ACh and stimulate its receptor targets;[7] (iii) hybrids that contain CHI functionality and a second noncholinergic modality, e.g., MAO inhibitory activity, melatonin surrogates, or nitric oxide releasing capability.[8−10] A fourth recent strategy (iv) has been to develop selective inhibitors for BuChE. In contrast to AChE, no physiological role has been assigned to BuChE, nor has it a known endogenous substrate; for the present, it takes its name from butyrylcholine, a synthetic substance it hydrolyses exceedingly rapidly (BuChE was historically referred to as pseudocholinesterase, perhaps disparagingly). BuChE is found ubiquitously throughout the human body but is at high concentrations in the lung, liver, and serum. This distribution pattern points to a role in primary metabolism, possibly in protecting the organism from agents that might inhibit the pivotal functions of AChE. Indeed, BuChE has a prominent role in the metabolism of ester drugs and in the activation of ester prodrugs. There are also suggestions that it may be involved in lipoprotein regulation.[11] Evidence for the involvement of BuChE in AD and support for its role as a drug target may be summarized as follows: (i) the nullizygous (AChE −/−) mouse while having a clear phenotype appears to have normal CNS function, indicating at least a compensatory role for BuChE in the CNS;[12] (ii) while synaptic AChE levels decrease to 10−15% of normal during AD progression, BuChE activity is maintained or even increased;[13] (iii) post mortem tissue analysis on AD patients shows a high level of BuChE in the hallmark lesions of AD[14] (although it might well have a protective role here); (iv) in rats, the selective BuChE inhibitor cymserine causes elevation of acetylcholine and augments long-term potentiation and learning.[15] A notable feature of that study was the absence of peripheral side effects that are associated with AChE inhibitors.

We reported previously that isosorbide esters tend to undergo very rapid hydrolysis in the presence of mammalian esterases.[16−18] The aspirin ester of isosorbide mononitrate (ISMNA) is one of the few compounds reported that can act as an aspirin prodrug (at least in rabbit plasma) and it is a potent inhibitor of platelet aggregation.[16] This is because, in the case of ISMNA, hydrolysis at the aspirin ester group proceeds faster than at the neighboring acetyl group. We hypothesized that it might be possible to generate potent and selective inhibitors for the cholinesterases by replacing the aspirin group in ISMNA with a carbamate functionality while retaining the isosorbide-5-nitrate group as illustrated in Figure 1b. The 5-nitrate appeared to us to be an important recognition feature for esterase complementarity. In this paper, we report on the pattern of enzyme inhibition by isosorbide-2-carbamate-5-nitrates and then isosorbide2-carbamate-5-alkyl and -aryl esters. Some of the compounds in the latter

* To whom correspondence should be addressed. Phone: +353-1-896 2795. Fax: +353-1-896 2793. E-mail: gilmerjf@tcd.ie.

[†] School of Pharmacy and Pharmaceutical Sciences, Trinity College.

[‡] School of Science, Athlone Institute of Technology, Westmeath, Ireland.

[a] Abbreviations: AChE, acetylcholinesterase; ATCI, acetylthiocholine iodide; BTCI, butyrylthiocholine iodide; BuChE, butyrylcholinesterase; DCC, dicyclohexylcarbodiimide; DTNB, 5,5′-dithiobis-(2-nitrobenzoic acid); *hu*BuCHE, human butyrylcholinesterase; ISMN, isosorbide-5-mononitrate; ISMNA, isosorbide mononitrate aspirinate; MAO, monoamino oxidase; SAR, structure activity relationship, TBAF, tetrabutylammonium fluoride; TBDMS, tertbutyldimethylsilyl; TMS, tetramethylsilane.

10.1021/jm800564y CCC: $40.75
Published on Web 09/26/2008

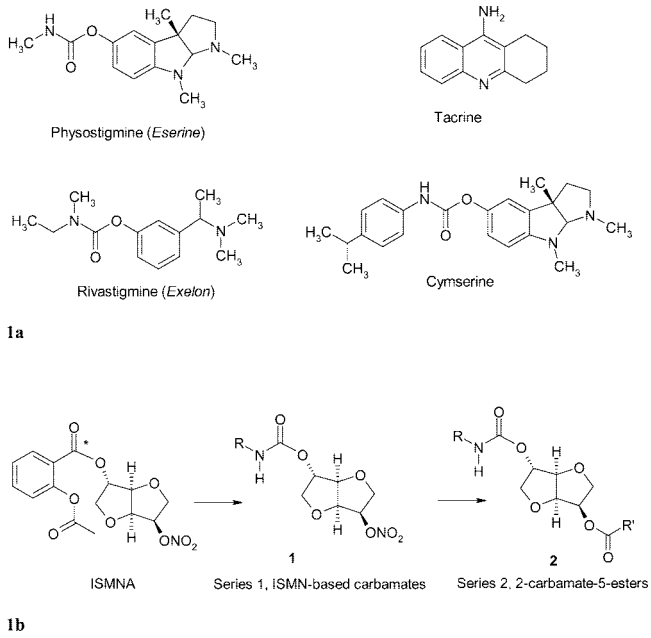

Figure 1. (1a) Carbamate inhibitors of the cholinesterases. (1b) Design strategy behind isosorbide-based carbamates.

group turned out to be among the most selective BuChE inhibitors reported. We also report preliminary kinetic and modeling data that provides an explanation for how these anomalous compounds work.

Chemistry

Isosorbide-2-carbamate-5-nitrates (series **1**, Figure 1b) were obtained by direct carbamylation of ISMN with the appropriate isocyanate in DCM in the presence of a triethylamine. The 2-carbamate-5-ester compounds of series **2** were obtained by removal of the nitrate under reductive conditions (H_2, Pd/C) and esterification with a series of commercially available acid chlorides. Where an acid chloride for a desired ester was not available, the acid itself was used instead with DCC/DMAP coupling (Scheme 1). In a few cases, acylation of the 2-carbamate nitrogen was found to compete with 5-esterification, and it proved difficult to get useful amounts of the target ester. In these cases, the order of carbamylation and esterification was reversed. ISMN was TBDMS-protected, the 5-nitrate removed, and then the 5-position esterified (Scheme 1). The 2-TBDMS group was then removed (TBAF) and the carbamate introduced as described already.

Enzyme Inhibition—SAR. Candidate inhibitors were evaluated using Ellman's spectrophotometric determination of cholinesterase activity with either human plasma or purified BuChE from human plasma.[19] For AChE activity, electric eel enzyme was used because this has quite similar active site structure to the human enzyme. Initially, the assumption was made that the inhibitors would act through carbamylation of the enzymes because their design was based on supersubstrates for *hu*BuChE (Figure 1b). Carbamate inhibition can be considered a two-step process with an initial rapidly established reversible interaction being followed by a slower covalent reaction between enzyme and inhibitor, forming an enzyme carbamate adduct.[20] The carbamate adduct hydrolyses slowly, liberating the free enzyme. The slow recovery of enzyme activity provides the fundamental kinetic distinction between carbamate inhibitors and ester substrates. Each stage of the carbamate inhibition and hydrolysis process can be influenced by structural features of the inhibitor.[20] IC_{50} values determined at a single time point are a composite value, reflecting the initial equilibrium as well as the rates of the carbamylation and decarbamylation steps and they are a generally used global measure of carbamate potency: *E*/*I* incubation times of 15−30 min are typical in the literature.[21−23] Inhibitory potency was determined in this study following incubation of the enzyme and test compound for 30 min. Several of the more potent compounds were also tested at 60 min with no significant shift in potency. Inhibition was initially evaluated at 100 μM with IC_{50} values estimated only for compounds showing significant inhibition (Table 1). The 5-nitrate compounds (series **1**) generally exhibited low micromolar potency toward BuChE with no significant inhibition of AChE at 100 μM. Potency increased in the series from methyl, ethyl, propyl, to butyl carbamate; the cyclohexyl carbamate had similar potency to the ethyl carbamate. The phenyl carbamates **1 g**−**k** were moderate inhibitors of both cholinesterases with slight preference in some cases for AChE. The most potent compound in the nitrate series was the 2-benzylcarbamate **1f** with an IC_{50} of 50 nM and >2000 fold selectivity for BuChE. When the benzyl group was maintained but the nitrate removed (leaving the isosorbide-5-position unsubstituted, **3**), there was a 74-fold drop in potency as well as selectivity (3.7 μM) although not because of any significant increase in potency toward AChE. Clearly, the 5-subsituent has a marked effect on inhibitory potency toward BuChE. It was therefore decided to explore 2-benzylcarbamates variously substituted at the 5-position with aryl and alkyl esters. The acetyl, propionyl, valeryl, and cyclopropyl ester compounds (**2a**−**e**) were moderately potent but selective inhibitors of BuChE. The cyclopentyl ester was the most potent of the alkyl ester compounds with an IC_{50} of 5.8 nM for BuChE and 975-fold selectivity over AChE. The 5-benzoate ester (**2i**) was the most potent compound in this study and the most selective BuChE inhibitor reported with an IC_{50} ratio of >63000 over electric eel AChE (4.3 nM/272 μM). When purified human erythrocyte AChE was used instead, the IC_{50} dropped a little to 221 μM and the selectivity ratio to 51000. The nicotinate esters **2j**−**k** were prepared as potentially more water soluble analogues, but they were around 20-fold less potent and selective than the corresponding benzoate. The influence of the ionisability of the pyridine ring on BuChE affinity or turnover was evaluated by measuring the IC_{50} at pH values in the range 6−8, the typical Ellman pH. The potency was found to be pH invariant in this range. A number of larger esters were prepared in order to test the hypothesis that in the case of BuChE, the isosorbide-5-ester group is accommodated by a large pocket or possibly back up the main active site channel. It was found that the benzoate ester could be replaced by 1- or 2-naphthoyl or biphenyl esters (**2l**−**n**) with little loss in potency. The cinnamate (**2o**) and coumarin (**2q**) esters were, however, significantly less potent and the heptyloxybenzoate ester (**2p**) quite inactive (IC_{50} 2.8 μM). Having used the 2-benzyl carbamate to probe for the optimal 5-ester, we now maintained the 5-benzoate group but changed the 2-carbamate group. The 5-benzoate-2-methylcarbamate (**2r**), -2-(3,4-dichlorophenylcarbamate) (**2s**), and 2-butylcarbamate (**2t**) compounds were significantly more potent than their nitrate analogues (**1a**, **1j**, and **1d**) as expected, but clearly in this panel of possible acyl groups, a benzyl carbamate is optimal in the 2-position and a benzoate ester at the 5-position.

Enzyme Inhibition—Mode. The relationship between inhibitory potency and assay substrate concentration was surveyed initially in a classical way in order to determine the mode of inhibition. Substrate hydrolysis velocity was proportional to

Scheme 1. Showing the Synthesis Routes to Candidate Inhibitors[a]

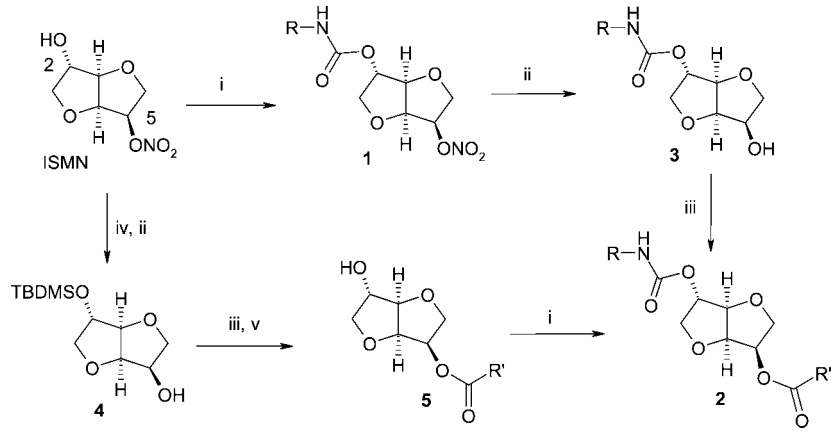

[a] (i) Isocyanate, pyridine or Et_3N/DMAP, DCM, 40 °C, 2 h; (ii) Pd/C, H_2, EtOAc, 12 h, RT; (iii) R′(CO)Cl, DMAP, Et_3N, DCM, RT, 8 h or R′C(O)OH, DCC, DMAP, DCM, RT, 8 h; (iv) TBDMSCl, imidazole, DMAP, DCM, 2 h, RT; (v) TBAF, THF, RT, 15 min.

Table 1. Carbamate Test Compounds along with Inhibition Data and Selectivity for BuChE and AChE[a]

	BuChE		AChE		
compd	%[b]	IC_{50} (μM)[c]	%[b]	IC_{50} (μM)[c]	selectivity[d]
series **1**, R=					
1a −methyl	82	5.1 (2.2−11.8)	67	17.2 (6−31)	
1b −ethyl	73	3.9 (1.6−9.7)	1		
1c −propyl	93	0.639 (0.66−1.2)	1	1520 (1300−1700)	2383
1d −butyl	92	0.894 (0.65−1.23)	32	1440 (1010−3300)	1610
1e−cyclohexyl	99	2.5 (1.7−3.4)	30		>40
1f −benzyl	96	0.051 (0.4−0.7)	35		>2000
1g −(3-trifluormethylphenyl)	10		12		
1h −phenyl	37		23		
1i −(2-chlorophenyl)	11		24		
1j −(3,4-dichlorophenyl)	28		78	9.9 (7.9−12.3)	
1k −(3-chlorophenyl)	11		24		
series **2**, R=Bn, R′=					
2a−acetyl	97	4.1 (3−5)	12		>25
2b−propionyl	97	0.98 (0.8−1.21)	5		>100
2c−valeryl	95	0.7 (0.52−0.94)	4		>142
2d−cyclopropyl	97	0.334 (0.25−0.44)	55		~300
2e−cyclopentyl	99	0.006 (0.001−0.0012)	88	56.3 (29−79)	9383
2f−triflate	85	0.359 (0.15−0.88)	6		>278
2g−mesylate	9.8		3		
2h−tosylate	25		66		
2i−benzoate	99	0.0043 (0.001−0.007)	21	272.5 (210−354)	63,255
2j−nicotinate	99	0.057 (0.049−0.068)	33		1754
2k−isonicotinate	97	0.088 (0.074−0.106)	24		
2l −(1-naphthoyl)	99	0.028 (0.025−0.032)	86	37.6 (21−69)	1342
2m −(2-naphthoyl)	100	0.032 (0.022−0.048)	80	43.4 (26−71)	1367
2n−biphenyl	99	0.012 (0.01−0.015)	89	51.6 (28−75)	4187
2o−cinnamate	96	0.137 (0.103−0.183)	82	55.9 (52−60)	~729
2p−(4-hepyloxy-)benzoate	80	2.8 (2.2−3.2)	21		35
2q−coumarin ester	100	0.073 (0.06−0.08)	81	60.4 (41−81)	821
R′, benzoate, R, carbamate					
2r−2-methycarbamate−	93	0.669 (0.541−0.768)	54		~150
2s −3,4-dichlorphenyl	38		70		
2t−2-butyl	99	0.072 (0.031−0.163)	31		1389
3−2-benzylcarbamate-5-OH	95	3.7 (3.3−4.1)	15		>27
eserine		0.028 (0.011−0.041)		0.103 (0.61−0.17)	3.7
iso-OMPA		0.733 (0.555−0.953)		2.5 (0.9−3.7)	3.41
BW284c51		255 (180−362)		0.063 (0.05−0.09)	2.5e-4

[a] All experiments performed in triplicate. [b] Inhibition % was determined at 100 μM inhibitor concentration. [c] IC_{50} values are expressed with the 95% confidence interval. [d] Selectivity was estimated by dividing the IC_{50} for AChE by the IC_{50} for BuChE. In cases where there was negligible inhibition of AChE at 100 μM and the IC_{50} was not determined, the selectivity is stated to be greater than the value obtained using 100 μM instead of the IC_{50}.

substrate concentration with increasing V_{max} values. Hydrolysis velocity was inversely proportional to inhibitor concentration consistent with a competitive mode of inhibition. However K_M values shifted only slightly. Double reciprocal plots yielded increasing slopes and intercepts, indicating mixed inhibition. Secondary replots of Lineweaver−Burk and Dixon data further indicated a significant amount of noncompetitive inhibition. This pattern can be observed when a reversible model is applied to pseudoirreversible inhibitors, and the assay is to a large extent measuring residual enzyme activity after carbamylation has already occurred. Therefore, the time dependence of inhibition was evaluated by sampling enzyme activity at successive time points immediately after introducing the inhibitor and then substrate. The experiment was performed repeatedly at increas-

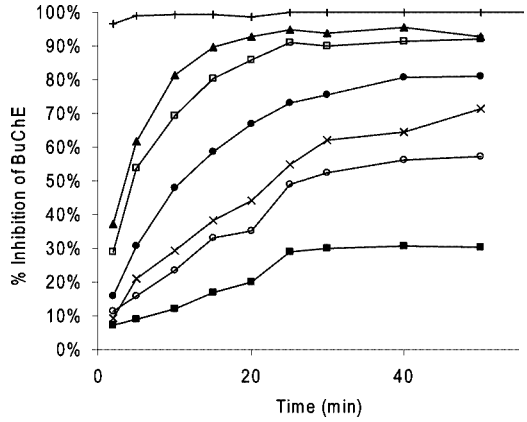

Figure 2. Percentage inhibition of *hu*BuChE by **2i** as a function of time at a BTCI concentration of 0.5 nM and inhibitor concentrations of 1.25 mM (+), 333 nM (▲), 250 nM (□), 125 nM (●), 83 nM (×), 62.5 nM (○), 50 nM (■).

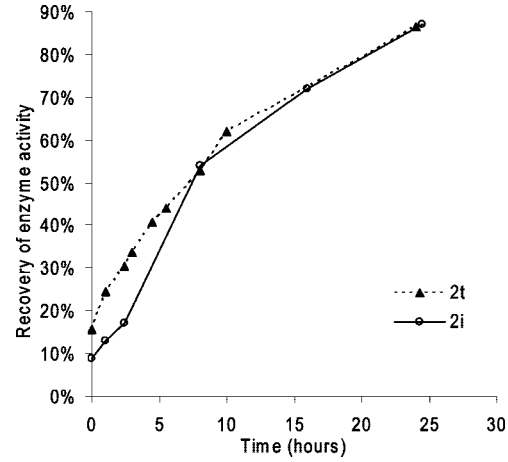

Figure 3. Recovery of purified *hu*BuChE enzyme activity following treatment with compound **2i** and **2t** and dilution.

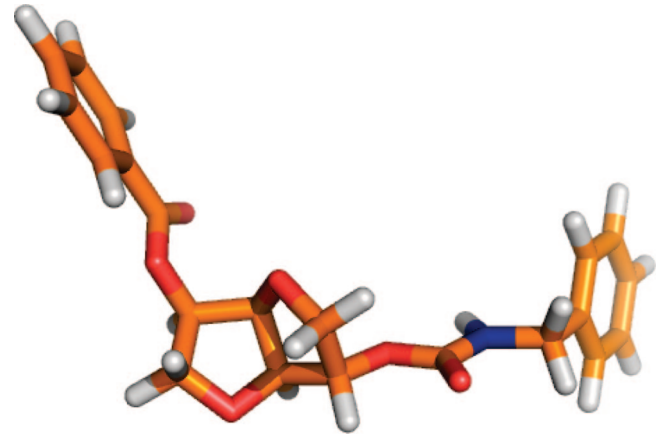

Figure 4. Conformation for compound **2i** produced using a stochastic search procedure followed by energy minimization using the MMFF94s force field in MOE. The 5-ester group is *endo* to the V-shaped ring, whereas the 2-carbamate is *exo*.

ing inhibitor but fixed substrate concentrations. The disappearance of enzyme activity for compounds **1f**, **2i**, and **2t** was time-dependent at low concentration but apparently immediate at high concentration. At intermediate−low concentration, the disappearance was first order and proportional to inhibitor concentration as shown in Figure 2 for **2i**. The IC_{50} values for **2i** determined at 60 min (3.6 nM (1.3−9.7)) was similar to the 30 min value. Further experiments were performed at fixed inhibitor concentration but increasing substrate concentration in the range 0.5−10 mM. The disappearance of enzyme activity was again time-dependent and the extent of inhibition at maximal inhibition was inversely proportional to substrate concentration, indicating competitive inhibition. When the carbamylation experiment was repeated for **2i** in the presence of edrophonium, a reversible active site directed inhibitor, there was a marked reduction in the rate and extent of inhibition.[24] Another relevant kinetic feature of carbamate inhibition is the slow regeneration of enzyme activity as the enzyme−carbamate adduct undergoes turnover. *hu*BuChE solutions were treated with compound **1f**, **2i**, or **2t** at a concentration giving 100% for two hours. Compound **2t** was selected because it gives rise to an enzyme−butyl carbamate adduct, whereas **1f** and **2i** generate enzyme−benzyl carbamates, albeit with different potencies. In the case of inhibitors **2i** and **2t**, the recovery of enzyme activity was measured following dilution to prevent reinhibition. Activity recovered slowly over 24 h but with similar rates (Figure 3). The **1f**-**E** solution was transferred to a dialysis bag and immersed in a buffered solution, which was then periodically changed as dialysis proceeded. In this case, there was significant residual inhibition up to 32 h.

In summary, the evidence for competitive cholinesterase carbamylation by the isosorbide-based carbamates is: (i) inhibition is time-dependent at low inhibitor concentration but independent of it at high concentration; (ii) the extent and rate of enzyme inhibition is substrate concentration dependent; (iii) inhibition is attenuated in the presence of the active-site dependent reversible inhibitor edrophonium; (iv) inhibition kinetics are first order at low concentration; (v) there is slow recovery of enzyme activity.

Modeling, Stability, and Structural Studies. Carbamate inhibitors of the cholinesterases are generally related to physostigmine, isolated from the *calabar* bean. They usually consist of an alkyl or aryl carbamate of a phenol with a distal amino group that is positively charged at physiological pH (Figure 1a). The compounds described here depart markedly from this pattern in being neutral (nonamino) and because they are derived from the secondary alcohol and pseudosugar, isosorbide. Isosorbide is V-shaped because of its *cis* ring junction with an angle of approximately 120 ° between two planar rigid rings. (Figure 4). The 2-α-OH group lies *exo* to the ring and the 5-*β* group *endo*. *Endo* substituents are directed into the V, *exo* groups outside it. Although this makes the 2-position more sterically accessible, in isosorbide, the 5-OH is activated because of an intramolecular H-bond to one of the ring oxygen atoms. In the 2-carbamate-5-esters, the 5-ester is directed orthogonal to the plane of isosorbide rings, whereas the 2-*exo* group points away from the system (Figure 4). In isosorbide diesters, the 2-group tends to undergo very rapid hydrolysis in human plasma. (This observation was critical to the carbamate design reported here.) The 5-*endo* ester is much less prone to hydrolysis (at least by butyrylcholinesterase) and in human plasma, isosorbide 2,5-diesters undergo hydrolysis almost exclusively at the 2-position, liberating the corresponding 5-monoester. For example, the half-life for isosorbide-2,5-dibenzoate at V_{max} concentration in 50% human plasma is 19 s with the exclusive liberation of isosorbide-5-benzoate.[18] The 5-benzoate product eventually decays with a half-life of 41 min. The dibenzoates do not undergo processing by AChE, indeed, substituted dibenzoates are moderately potent AChE inhibitors.[25]

To confirm the stability of the 5-ester under assay conditions, compound **2i** was incubated in 50% human plasma solution in

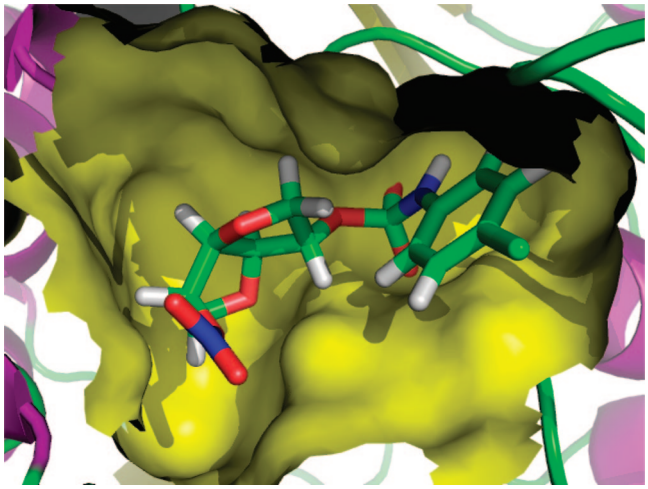

Figure 5. Compound **1f** docked within the active site gorge of *hu*BuChE with Connolly interaction surface in yellow and a Gaussian contact surface as a red mesh.

the range 10−100 μM. No hydrolysis occurred over several hours as measured by HPLC, and there was no apparent formation of either benzoic acid or isosorbide-5-benzoate, the carbamylation product. Enzyme−substrate interactions with the isosorbide-2-carbamate are preferred over enzyme-5-ester and the carbamate interaction is inhibitory, abolishing esterase activity. The failure to detect the carbamylation byproduct in this experiment is probably due to the negligible depletion of inhibitor by the tiny amount of enzyme present (BuChE is present in human plasma at about 5 mg/L with a mass of 86 kD per subunit).[26] Although isosorbide-5-esters are products of the pseudosubstrate carbamate interaction, they do not accumulate sufficiently in the inhibitory period to have influenced the inhibitory data. The isosorbide-5-benzoate ester product of compound **2i** is in any case a weak reversible inhibitor of BuChE (30% at 100 μM). The modeling and kinetic data for series **2** suggest that the 5-ester group promotes carbamylation by binding in the active site in orientations that are productive for enzyme carbamylation but not for 5-ester hydrolysis. BuChE is the most significant esterase in human plasma (at least in terms of activity). We can anticipate problems with the compounds in in vivo models because of nonspecific 5-ester hydrolysis by carboxylesterases present in other tissues that do not possess the same substrate or inhibitor/substrate as BuChE.[27] However, these observations are not relevant to interpretation of the BuChE−ligand interaction data presented here.

A modeling approach was used to further explore the nature of 5-ester interaction, the role of the 5-ester group in determining potency, and the basis for cholinesterase selectivity. Modeling of cholinesterase enzymes and their inhibitors has been aided greatly by the elucidation of the structures of enzyme−ligand complexes for both BuChE and its homologous enzyme, AChE.[28−30] The active sites of both enzymes are at the base of a gorge of some 20 Å depth in both cases.[31,32] On the basis of crystallographic studies, mutagenesis work, and radiolabeling studies, a number of subsites have been identified in the catalytic gorges that are typically involved in binding ligands, both substrates and inhibitors. While the residues that comprise these sites vary between BuChE and AChE, the overall structures are basically similar, and comparisons between the two uncover the origins of binding specificity and the basis of ligand selectivity for one enzyme over the other.

These enzymes are serine hydrolases, and a classic catalytic triad is formed with histidine and glutamate. In *hu*BuChE, these residues are Ser-198, His-438, and Glu-325. Other residues of note in BuChE are Trp-82, the principal residue of the cation-π site where the cationic head of choline substrates bind; the peripheral site residues, Asp-70 and Tyr-332, which bind ligands initially and help to orientate them appropriately to slide down the gorge and interact with the active site, and Glu-116, Glu-117, and Ala-199, which together form the oxyanion hole that stabilizes the negative charge on the carbonyl oxygen that develops subsequent to the nucleophilic attack by O-γ of the catalytic serine. The principal difference between the enzymes is the size of the acyl pocket. In AChE, the pocket is occluded by the aromatic groups of residues Phe-288 and Phe-290 (*Torpedo californica* AChE numbering is used throughout the text when referring to residues of AChE). In the larger BuChE channel, the acyl pocket is lined with the aliphatic residues Leu-286 and Val-288.

Kinetic studies indicated that inhibition by the isosorbide-based carbamates proceeds through serine carbamylation. This involves a tetrahedral intermediate that collapses to the carbamylated drug−enzyme adduct. While the transition state during a reaction process is associated with a first-order saddle point on the potential energy surface, this tetrahedral intermediate is an energy minimum on the overall surface and can thus be modeled using classical force field-based methods as described by Gao et al.[33]

Isosorbide inhibitors of BuChE were modeled in the active site of the enzyme as this tetrahedral intermediate, allowing us to draw structural conclusions regarding the basis of relative inhibitor activity. The approach has the virtue of limiting the potential containment volume of the ligand and has been used to model cholinesterase inhibitors previously.[34] It is structurally very similar to the reversible Michaelis complex formed upon initial binding and will indicate the likelihood of initial binding in a manner that is appropriate for carbamylation.

Modeling of the isosorbide-based inhibitors was based on the 2.0 Å resolution crystal structure of *hu*BuChE. (PDB entry 1p0i).[32] When BuChE was crystallized and its structure established, it was noted that the catalytic Ser-198 was bound to an unidentified moiety that was ultimately modeled as butyrate. Apparently, the presence of this butyrate fragment was essential for crystallization. The butyrate was bound to the serine residue in a tetrahedral configuration, with one oxygen atom orientated toward the oxyanion hole. The second oxygen atom points toward Trp-82, while the butyryl chain points toward the acyl pocket. The butyrate fragment could thus be used as a template for the tetrahedral intermediate involved in carbamylation. The assignment of directionality for the other functional groups was based on the positioning of similar groups in crystal structures of other enzyme−ligand complexes. The bulky isosorbide ester fragment could be orientated toward Trp-82, while the carbamate side chain could be directed toward the acyl pocket; similar placement of side chains could be observed in the crystal structures of rivastigmine and trimethylammonium trifluoroacetophenone with AChE (PDB codes 1gqr and 1amn, respectively).[29,35] The inhibitors were built in situ within the enzyme active site using the butyrate fragment as a template and placing each group at the appropriate binding subsite. A tethered minimization procedure gave rise to the models, two of which are presented in Figures 5 and 6.

The general activity of the inhibitor series could be explained by the fact that the isosorbide moiety, when the attached carbamate is bound by the catalytic serine, closely lines the base of the gorge (Figure 5) while orientating the two groups at the 2- and 5-position toward appropriate pockets. The relative

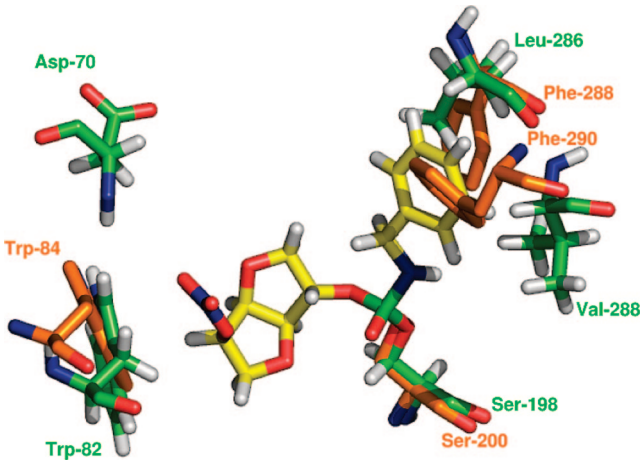

Figure 6. Compound **1f** covalently bound to *hu*BuChE. Residues Ser-200, Trp-84, Phe-288, and Phe-290 of *Tc*AChE are also shown, having been overlaid from the AChE structure from PDB code 1EA5. AChE residues are shown in orange; BuChE residues are green and the ligand yellow.

potencies of the different compounds in Table 1 could be explained by the extent to which the functional groups, permitting interactions with various residues of the active site gorge.

In series **1**, the carbamate group was altered while a nitrate group was maintained at the 5-position of isosorbide. The carbamate function was orientated toward the acyl pocket, and it was the differential interaction of the various groups with the residues at this position that gave rise to the variable potencies of these compounds. Smaller carbamate compounds tended to be poorer inhibitors of BuChE, largely because they failed to fully occupy the large pocket formed by residues Leu286 and Val288. Thus the methyl and ethyl carbamates were relatively poor inhibitors, but potency increased for propyl and butyl carbamates as the longer chains could fit better within the gorge. The phenyl carbamates were also poor inhibitors of BuChE in general because they similarly could not fill the pocket. The extra methylene group in the benzyl carbamate functional group allowed extension of the side chain into the acyl pocket, however, and the formation of $\sigma-\pi$ interactions between the aromatic ring of the ligand and the aliphatic side chains of the surrounding residues. These findings were borne out within the models: the interaction energy between the benzyl carbamate compounds and BuChE was predicted as being almost 8 kcal·mol^{-1} more favorable than the methyl carbamate and 3 kcal·mol^{-1} more favorable than the phenyl carbamate. The acyl pocket of AChE is larger and therefore less able to cope with large carbamate side chains. Phenyl carbamates tend to interact well with the aromatic side chains of Phe288 and Phe290, a fact that has been documented previously for a number of compounds such as phenserine. Extended side chains at this site tend to favor BuChE selectivity, hence the BuChE selectivity of benzyl carbamate compounds. This effect is demonstrated in Figure 6.

Modification of the group at the 5-position (series **2**) gave rise to compounds of variable potency. In the models that were prepared, the fragments at the 5-position pointed upward toward the gorge entrance, aligned with Trp-82 at the so-called cation-π site and toward the peripheral site residues at the lip of the gorge. The 5-nitrate group is relatively small and relatively few interactions were evident between this group and residues of the catalytic gorge. Its presence was still important; compound **1f** is substantially more potent than compound **3**, and this was predicted by quantitative analysis, which suggested a 7 kcal·mol^{-1} difference in binding energy between the two compounds in favor of compound **1f**. However, the incorporation of a variety of ester derivatives served to significantly increase potency. Models suggested that compound **2i** should bind more avidly to BuChE than **1f** by a factor of 8 kcal·mol^{-1}. This is principally due to the increased interaction with Trp82, the principal residue of the cation-π site. Longer chain esters could also be accommodated due to the general orientation of the 5-group pointing upward toward the gorge entrance. The biphenyl ester, for example, can interact not only with Trp82 but also Trp430, compensating for its steric bulk. Its predicted binding energy was then 1 kcal·mol^{-1} less than compound **2i**.

Table 2. Predicted Binding Affinity for a Selected Range of Inhibitors to BuChE Relative to Compound **2i**

compd	affinity (kcal·mol^{-1})
2n	−0.656
2t	−4.39
2j	−0.166
2r	−10.997
1a	−16.212
1h	−10.693
1f	−8.340
3	−14.562

The predicted binding energies of a number of the compounds, relative to the most potent inhibitor in the group, compound **2i**, are shown in Table 2.

Because the models described below are inherently biased toward the starting pose prior to minimization, a covalent docking procedure was also carried out in order to examine whether the placement of the molecules in the active site was optimal. This was achieved using the Autodock 3 program.[36] In this case, the ligand could dock within the gorge in any orientation without bias toward starting structure. Compound **2i** was docked within the active site gorge of *hu*BuChE. When the results were clustered, the largest of only four molecular clusters contained molecules docked in the described orientation. It was satisfying that the docked poses were generally similar to that produced using the minimization protocol despite the fact that the protein was rigid in this protocol. The simple and fast minimization procedure could apparently produce reliable models of the inhibitors that were replicated by the more rigorous docking approach (Figure 7).

Conclusion

Isosorbide-2-carbamate-5-nitrate and -benzoate esters are highly potent and selective inhibitors of *hu*BuChE. They are structurally distinct from established carbamates, being uncharged and derived from a secondary alcohol. Their neutrality is likely to be important to their potential utility. Central and peripheral BuChE have similar structures at the subunit level so that inhibitors of plasma BuChE ought to act as inhibitors of central BuChE, provided they cross the blood−brain barrier. The compounds act as competitive pseudosubstrates with time-dependent but reversible inhibition. Molecular models indicate that they bind with the carbamate functionality pointed into the acyl pocket and the 5-ester group directed back up the cholinesterase channel. The 5-position shows some tolerance to substitution, which might allow for tuning of pharmaceutical characteristics or the introduction of new pharmacological modalities. Compounds **2i** and **2t** are being evaluated in clinically relevant models of learning and memory in aged mice.

Experimental Section

Chemistry. Infrared (IR) spectra were obtained using a Perkin-Elmer 205 FT Infrared Paragon 1000 spectrometer. Band positions

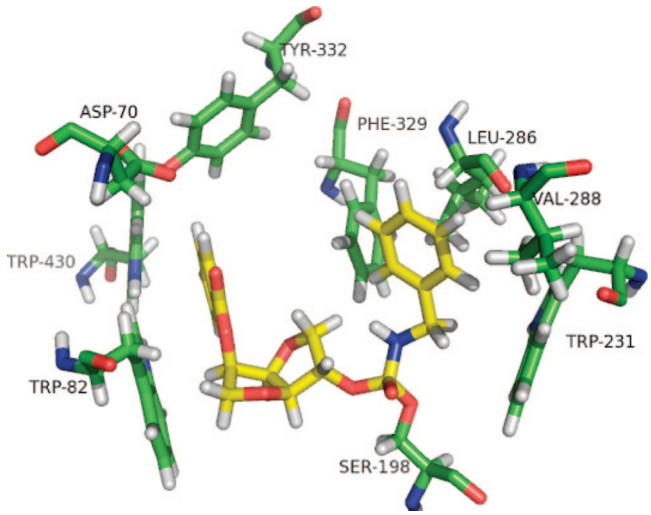

Figure 7. Compound **2i** modeled as the tetrahedral acylation intermediate in the BuChE active site using Autodock 3.

are given in cm^{-1}. Solid samples were obtained by KBr discs, and oils were analyzed as neat films on NaCl plates. ^1H and ^{13}C spectra were recorded at 27 °C on a Brucker DPX 400 MHz FT NMR spectrometer (400.13 MHz ^1H, 100.61 MHz ^{13}C) or a Brucker AV600 (600.13 MHz ^1H, 150.6 MHz ^{13}C) in either $CDCl_3$ or $(CD_3)_2CO$ with TMS as internal standard. In $CDCl_3$, ^1H spectra were assigned relative to the TMS peak at 0.0 ppm, and ^{13}C spectra were assigned relative to the middle $CDCl_3$ triplet at 77.00 ppm. In $(CD_3)_2CO$, ^1H spectra were assigned relative to the $(CD_3)_2CO$ peak at 2.05 ppm, and ^{13}C spectra were assigned relative to the $(CD_3)_2CO$ at 29.5 ppm. Coupling constants were reported in hertz (Hz). HRMS was performed using a Micromass mass spectrophotometer with electrospray ionization at the School of Chemistry, Trinity College Dublin. Elemental analyses were performed at the Microanalytical Laboratory, Department of Chemistry, University College Dublin. Flash chromatography was performed on Merck Kieselgel (particle size: 60 mm).

Isosorbide-2-(butylcarbamate)-5-mononitrate (1d). ISMN (0.7852 g, 4 mmol) was dissolved in dry pyridine (5 mL). Butyl isocyanate (mol wt 99.13 g/mol, $d = 0.880$ g/mL, 8 mmol, 0.79304 g, 0.9 mL) was added and the mixture heated at 100 °C for 1 h. The mixture was cooled and methanol (10 mL) added to remove excess isocyanate. The mixture was then heated for further 10 min at 100 °C, cooled to room temperature, poured into ice−water, and stirred. The precipitate was collected and crystallized from hot methanol to yield 0.69 g of a white crystalline product (59.3%): mp 101.7 °C. ^1H NMR δ ($CDCl_3$): 0.91−0.95 (t, 3H, $J = 7.8$ Hz.), 1.32−1.1.39 (m, 2H), 1.45−1.51 (q, 2H, $J = 7.8$ Hz), 3.16−3.21 (q, 2H, $J = 7$ Hz), 3.88−3.3.92 (m, 1H), 3.96−4.06 (m, 3H), 4.49−4.50 (d, 1H, $J = 5.3$ Hz,), 4.79 (s, 1H), 4.95−4.97 (t, 1H, $J = 5.3$ Hz), 5.17−5.18 (d, 1H, $J = 2.6$ Hz), 5.3−5.35 (m, 1H). ^{13}C NMR ppm ($CDCl_3$): 13.2, 19.39, 31.4, 40.3, 68.7, 73.3, 77.1, 80.9, 80.9, 86.34, 154.6. Anal. ($C_{11}H_{18}N_2O_7$) C, H, N.

Isosorbide-2-(benzylcarbamate)-5-mononitrate (1f). A white crystalline product (47.3%): mp 93.4 °C, $[\alpha]_D$ +99.01 °C. ^1H NMR δ ($CDCl_3$): 3.88−3.91 (m, 1H), 3.96−4.07 (m, 3H), 4.36−4.38 (d, 2H, $J = 6$ Hz), 4.50−4.51 (d, 1H, $J = 4.8$ Hz), 4.94−4.96 (t, 1H, $J = 5.2$ Hz), 5.20−5.21 (d, 1H, $J = 2.8$ Hz), 5.23 (s, 1H), 5.33−5.36 (m, 1H), 7.28−7.38 (m, 5H). ^{13}C NMR ppm ($CDCl_3$): 69.6, 74.1, 77.2, 78.23, 81.76, 81.85, 87.14, 127.95, 128.07, 129.2, 138.42, 155.54. Anal. ($C_{14}H_{16}N_2O_7$) C, H, N.

Isosorbide-2-phenylcarbamate-5-mononitrate (1h). A white crystalline product (22%): mp 156.6 °C, $[\alpha]_D$ +81.0 °. ^1H NMR δ ($CDCl_3$): 3.9 (m, 1H), 4.0 (m, 2H), 4.1 (d, 1H), 4.5 (d, 1H, $J = 4.9$ Hz), 5.0 (t, 1H, $J = 4.9$ Hz), 5.3 (d, 1H, $J = 3$ Hz), 5.4 (m, 1H), 6.7 (s, 1H), 7.1 (t, 1H), 7.3 (m, 4H). ^{13}C NMR ppm ($CDCl_3$): 69.31, 73.59, 78.02, 81.29, 81.53, 86.66, 118.72, 123.93, 129.17, 137.24, 152.05. Anal. ($C_{13}H_{14}N_2O_7$) C, H, N.

Isosorbide-2-benzylcarbamate (3). 2-(Benzylaminocarbonyloxy-)-5-*O*-nitro-1,4:3,6-dianhydro-D-glucitol **1f** (mol wt 324.29 g/mol, 46.25 mmol, 15 g) was dissolved in ethyl acetate:methanol 1:1 (100 mL) in a 250 mL round-bottom flask. A spatula tip-full of 10% palladium on activated carbon was added to the solution. Air was expelled from the flask, and the mixture was kept under an atmosphere of hydrogen gas and stirred for 24 h. The solvent was evaporated under vacuum, and the crude product was dissolved in DCM and filtered through silica. The filtrate was collected and evaporated under vacuum to yield 12.60 g as a white crystalline product (97.5%). mp 76.0 °C. ^1H NMR δ ($CDCl_3$): 2.67 (d, 1H, $J = 7.03$ Hz), 3.57 (dd, 1H, $J = 5.53$, 8.54 Hz), 3.90 (dd, 1H, $J = 6.03$, 9.54 Hz), 4.00 (dd, 1H, $J = 3.51$, 10.54 Hz), 4.10 (d, 1H, $J = 10.45$), 4.31 (m, 1H), 4.38 (d, 2H, $J = 6.03$ Hz), 4.51 (d, 1H, $J = 4.01$ Hz), 4.61 (t, 1H, $J = 4.77$ Hz), 5.17 (m, 1H), 5.22 (d, 1H, $J = 3.01$ Hz), 7.23−7.40 (m, 5H). ^{13}C NMR ppm ($CDCl_3$): 44.70 (CH_2), 71.8, 73.04, 73.38, 78.39, 81.46, 85.25, 127.13, 127.23, 128.30, 137.6, 154.69. Anal. ($C_{14}H_{17}NO_5$) C, H, N.

Isosorbide-2-benzylcarbamate-5-cyclopropanoate (2d). A white crystalline product (265.2 mg, 85.2%): mp 96 °C. ^1H NMR δ ($CDCl_3$): 0.87−0.98 (m, 2H), 1.04 (m, 2H), 1.70 (m, 1H), 3.80 (dd, 1H, $J = 5.52$, 9.54 Hz), 3.95 (dd, 1H, $J = 6.$ 03, 9.54 Hz), 3.98−4.08 (m, 2H), 4.37 (d, 2H, $J = 6.02$ Hz), 4.52 (d, 1H, $J = 4.51$ Hz), 4.79 (t, 1H, $J = 4.77$ Hz), 5.14 (q, 1H, $J = 5.52$, 11.54 Hz), 5.17−5.27 (m, 2H), 7.22−7.40 (m, 5H). ^{13}C NMR ppm ($CDCl_3$): 44.64, 69.74, 73.25, 73.48, 78.09, 80.27, 85.52, 127.10, 127.17, 128.3, 137.65, 154.81, 173.93. Anal. ($C_{18}H_{21}NO_6$) C, H, N.

Isosorbide-2-benzylcarbamate-5-cyclopentanoate (2e). A white crystalline compound (81.9%): mp 94 °C. ^1H NMR δ ($CDCl_3$): 1.53−2.00 (m, 8H), 2.83 (m, 1H), 3.73 (dd, 1H, $J = 5.02$ and 10.03 Hz), 3.89−4.06 (m, 3H), 4.39 (d, 2H, $J = 6.02$ Hz), 4.50 (d, 1H, $J = 4.51$ Hz), 4.81 (t, 1H, $J = 5.02$ Hz), 5.08−5.18 (m, 2H), 5.20 (d, 1H, $J = 3.01$ Hz), 7.22−7.40 (m, 5H). ^{13}C NMR ppm ($CDCl_3$): 25.35, 25.37, 29.43, 29.73, 43.04, 44.65, 70.12, 73.05, 73.21, 78.06, 80.29, 85.62, 127.10, 127.19, 128.28, 137.61, 154.79, 175.78. Anal. ($C_{20}H_{25}NO_6$) C, H, N.

Isosorbide-2-(benzylcarbamate)-5-benzoate (2i). Compound **3** (0.6027 g, 2 mmol) was dissolved in dry pyridine (5 mL), and the solution was cooled to −5 °C using a salt/water bath. Benzoyl chloride (mol wt 140.57 g/mol, $d = 1.211$ g/mL, 5 mmol, 0.56 mL) was added. The mixture was allowed to come to room temperature, and stirring was continued for 22 h. The mixture was added to ice−water (approx 200 mL), and the precipitated solid was filtered. The resultant solid was taken up in chloroform (15 mL) washed first with water (10 mL) then with saturated brine solution (10 mL), dried with anhydrous sodium sulfate (10 g), filtered into a round-bottomed flask, and evaporated under reduced pressure. The resultant semisolid was recrystallized from hot ethanol to yield 0.74 g of a white crystalline product (96.1%): mp 76.0 °C, $[\alpha]_D$ +13.45 °C. ^1H NMR δ (DMSO): 3.84−3.85 (s, 2H), 3.85−3.97 (m, 2H), 4.18−4.20 (d, 2H, $J = 6.4$ Hz), 4.45−4.46 (d, 1H, $J = 5.2$ Hz), 4.88−4.91 (t, 1H, $J = 5.6$ Hz), 5.03 (s, 1H), 5.36−5.38 (t, 1H), 7.23−7.33 (m 5H), 7.53−7.57 (m, 2H), 7.66−7.70 (m, 1H), 7.97−8.01 (m, 3H). ^{13}C NMR ppm (DMSO): 44.10, 70.89, 73.08, 74.79, 77.86, 81.04, 86.29, 127.16−127.37, 128.63, 129.19, 129.56−129.65, 133.86, 139.89, 155.8, 165.30. Anal. ($C_{21}H_{21}NO_6$) C, H, N.

Isosorbide-2-benzylcarbamate-5-nicotinate (2j). To a solution of 2-*O*-(*t*-(butyl)-dimethylsilyl-)-1,4:3,6-dianhydro-D-glucitol **4** (mol wt 260.40 g/mol, 1.1521 mmol, 300 mg) in dry THF (50 mL) was added 1.25 mol equiv of anhydrous nicotinoyl chloride hydrochloride (mol wt 178.05 g/mol, 1.4400 mmol, 256.4 mg). The mixture was kept under an atmosphere of nitrogen and stirred at room temperature for 15 min. To the mixture was added four mol equiv of triethylamine, and stirring was continued for a further 24 h. The solvent was evaporated under vacuum to give a white residue, which was dissolved in a saturated aqueous solution of Na_2CO_3 (25 mL) and extracted with DCM (3 × 25 mL). The collected organic portions were dried over anhydrous sodium sulfate (5 g) and evaporated to dryness to give a clear oil. The oil was diluted with

THF (10 mL) and 1.1 mol equiv of TBAF (mol wt 261.47 g/mol, 0.7524 mmol, 196.7 mg, 0.7524 mL of a 1 M solution) was added, and the mixture was stirred at room temperature for 15 min. The solution was evaporated to dryness under vacuum giving a brown oil. DCM (10 mL) was added to the reaction vessel, and the solution was stirred at room temperature. To the mixture was added triethylamine (mol wt 101 g/mol, d 0.726 g/mL, 0.7515 mmol, 75.9 mg, 0.1047 mL), benzyl isocyanate (mol wt 133.15 g/mol, d 1.078 g/mL, 0.7515 mmol, 100.2 mg, 0.0929 mL), and DMAP (mol wt 122.17 g/mol, 0.2456 mmol, 30 mg). The mixture was heated to 105 °C for two hours. The mixture was cooled upon completion of the reaction, and methanol (10 mL) was added to remove excess isocyanate. The mixture was heated for a further 15 min at 105 °C and cooled to room temperature. All organic solvent was removed under vacuum giving a clear oil to which was added DCM (20 mL) and washed with 1 M HCl (20 mL), 5% $NaHCO_3$ (20 mL), and saturated brine solution (20 mL) and dried over anhydrous sodium sulfate (2 g). The solution was filtered into a round-bottomed flask, which was evaporated under vacuum to give a white crystalline compound. Purification by column chromatography using hexane and ethyl acetate (3:1 and 1:1) as eluent afforded **2j** as a white crystalline compound (187.7 mg, 42.3%): mp 136 °C, mol. ^{1}H NMR δ ($CDCl_3$): 3.93−4.07 (m, 4H), 4.37 (d, 2H, J = 6.03 Hz), 4.55 (d, 1H, J = 4.52 Hz, IsH-3), 4.94 (t, 1H, J = 5.02 Hz), 5.22 (d, 1H, J = 2.01 Hz), 5.39 (m, 2H), 7.20−7.37 (m, 5H), 7.38−7.48 (s, 1H), 8.32 (d, 1H, J = 7.53 Hz) 8.80 (s, 1H), 9.35 (s, 1H). ^{13}C NMR ppm ($CDCl_3$): 44.64, 70.17, 73.18, 74.50, 77.85, 80.44, 85.82, 123.12, 126.78, 127.0, 127.15, 128.25, 136.74, 137.65, 150.47, 153.23, 154.81, 165.36. Anal. ($C_{20}H_{20}N_2O_6$) C, H, N.

2-(Benzylaminocarbonyloxy-)-5-*O*-(1-naphthoyl)-1,4:3,6-dianhydro-D-glucitol (2l). A white crystalline product (86.8%): mp 126 °C. ^{1}H NMR δ ($CDCl_3$): 4.01−4.16 (m, 4H), 4.38 (d, 2H, J = 6.03 Hz), 4.61 (d, 1H, J = 4.52 Hz), 5.03 (t, 1H, J = 5.02 Hz), 5.11 (s, 1H), 5.26 (s, 1H), 5.51 (q, 1H, J = 5.53, 11.05 Hz), 7.23−7.40 (m, 5H), 7.50−7.60 (m, 2H), 7.65 (t, 1H, J = 7.28 Hz), 7.92 (d, 1H, J = 8.03 Hz), 8.07 (d, 1H, J = 8.03 Hz), 8.25 (d, 1H, J = 7.72 Hz), 8.96 (d, 1H, J = 8.53 Hz). ^{13}C NMR ppm ($CDCl_3$): 44.69, 70.23, 73.2, 74.11, 78.14, 80.56, 85.80, 124.06, 125.31, 125.85, 125.90, 127.11, 127.21, 127.47, 128.11, 128.30, 130.01, 130.95, 133.30, 133.36, 137.54, 154.77, 166.33. Anal. ($C_{25}H_{23}NO_6$) C, H, N.

Isosorbide-2-(methylcarbamate)-5-benzoate (2r). Colorless gum (0.52 g, 65%). ^{1}H NMR δ ($CDCl_3$): 8.02 (2H, d, J = 8.03 Hz), 7.55 (1H, t, J = 7.53 Hz), 7.42 (2H, t, J = 8.03 Hz), 5.36 (1H, d, J = 5.52 Hz), 5.15 (1H, s), 4.91 (1H, t, J = 5.02 Hz), 4.51 (1H, d, J = 5.02 Hz), 3.91 (4H, m,), 2.75 (3H, d, J = 4.52 Hz). ^{13}C NMR δ ($CDCl_3$): 165.45, 155.22, 132.85, 129.24, 128.96, 128.01, 86.29, 80.96, 80.49, 77.21, 73.13, 68.70, 27.00. HRMS**:** found, $(M - Na)^+$ = 330.0946; required, $(M - Na)^+$ = 330.0954.

Isosorbide-2-(butylcarbamate)-5-benzoate (2t). A white crystalline product; (10.2%): mp 81.7 °C, mol. ^{1}H NMR δ (DMSO): 0.8−0.9 (t, 3H), 1.2−1.3 (q, 2H), 1.33−1.38 (q, J = 2.4 Hz), 2.96−2.99 (q, 2H, J = 6.4 Hz), 3.82−3.83 (s, 2H), 3.89−3.97 (m, 2H), 4.41−4.43 (d, 1H, J = 5.2 Hz), 4.86−4.89 (t, 1H, J = 5.2 Hz), 4.99 (s, 1H), 5.36−5.39 (q, 1H, J = 4 Hz), 7.35−7.38 (t, 1H, J = 5.6 Hz), 7.53−7.57 (m, 2H), 7.66 (m, 1H), 7.9−8 (d, 2H). ^{13}C NMR ppm (DMSO): 13.97, 19.74, 31.75, 40.0, 70.87, 73.08, 74.79, 77.55, 81.02, 86.31, 129.18, 129.55, 129.6, 133.84, 155.53, 165.28. Anal. ($C_{18}H_{23}O_6N$) C, H, N.

Enzyme Studies. Cholinesterase activity was measured using the Ellman spectrophotometric method. *Hu*BuChE activity was measured in replicate samples using a 96-well plate reader. The total volume of test solution in each well was 250 μL. This consisted of 25 μL of plasma solution, 150 μL of phosphate buffer pH 8.0, 25 μL of DTNB solution (0.5 mM), and 25 μL of acetonitrile: distilled water (1:1). The 96-well plate was incubated for 30 min before 25 μL of BTCI solution (0.5 mM) was added, and the reaction was measured at 405 nm over 5 min using an Anthos bt2 plate reader. For the determination of AChE activity, 25 μL of electric eel AChE solution and 25 μL of ATCI solution were used instead of the plasma solution and BTCI solution. For determination of enzyme inhibition, 25 μL of an inhibitor solution was added to the test solution instead of the acetonitrile:water (1:1) solution. Inhibitors were added 30 min before determination of remaining enzyme activity. IC_{50} values were calculated using xlfit 4.0 software and GraphPad Prism 4.02 software. For carbamylation studies with compounds **2i** and **2t**, initial testing involved measuring cholinesterase activity at various [I] and [S] while incubating the enzyme and inhibitor over a 1 h period. Readings were obtained at 0, 5, 10, 20, 30, 40, 50, and 60 min with [E] = 1.2×10^{-3} mg/mL purifed *hu*BuChE, [DTNB] = 0.3 mM, [S] and [I] varied. The relevant amounts of buffer, inhibitor, and enzyme were mixed in a cuvette and allowed to incubate for the various time intervals. Once incubation was complete, the DTNB and substrate were added and the reaction was measured at 412 nm for 5 min. After completion of the above, the data was transformed so as to plot ln E/E_T versus time. The carbamylation experiments were repeated using compound **2t** at 1 mM (giving 100% inhibition) in the presence of the edrophonium (5 mM). The reversibility of carbamate inhibitors was determined by using dialysis or by dilution of the enzyme carbamate adduct and monitoring for recovery of activity. The dialysis experiments were performed using Visking dialysis tubing (Medicell International Ltd. supplied from Lennox Laboratory Supplies Ltd., Dublin) with an exclusion limit of 12000−14000 Da. The enzyme was mixed with inhibitor at a concentration giving 100% inhibition. Each experiment was performed in triplicate. Tubing was sealed at both ends using dialysis clips (Lennox Laboratory Supplies Ltd., Dublin). The samples were dialysed against buffer (1 L) at 37 °C, with samples being removed and assayed at intervals. The buffer was renewed at 4−6 h intervals. A control containing no inhibitor was treated and sampled in parallel with the samples. In the dilution experiments (compounds **2i** and **2t**), enzyme was incubated with sufficient inhibitor for at least 2 h to effect at least 90% inhibition. The mixture was then diluted 1000-fold in order to minimize the possibility of reinhibition by excess inhibitor. This dilution was made using phosphate buffer pH 8.0. The diluted sample was kept at 37 °C for the duration of the analysis, with aliquots being taken at defined time intervals and checked for BChE activity as described previously.

Stability Studies. Pooled plasma solutions (4 mL, 50%) were prepared by centrifugation of citrated human venous blood and dilution of the resultant supernatant with pH 7.4 phosphate buffer (2 mL). The pooled plasma sample gave normal adult BuChE activity. A 100 μL aliquot of compound **2i** in acetonitrile was added to plasma solution and then incubated (37 °C). Aliquots (250 μL) of the incubated mixture were withdrawn at appropriate intervals and transferred to 1.5 mL Eppendorf tubes containing 500 μL of 2% ZnSO4·7H20 in MeCN−H_2O (1:1) solution and 250 μL of acetonitrile. Samples were then vortexed for 30 s and centrifuged for 3 min at 10000 rpm. A 20 μL aliquot of the clear supernatant was analyzed by HPLC. A gradient method was used with a Waters ODS2 4.6 mm × 250 mm column and mobile phase consisting of phosphate buffer (pH 2.5):acetonitrile, 50:50, grading to 20:80 over 20 min. External standards of isorobide-5-benzoate, benzoic acid, and compound **2i** were used to confirm specificity. The eluent was monitored at 230 nm and peak identity and homogeneity confirmed by PDA analysis. The experiment was repeated five times in the range 1−100 μM.

Docking Studies. The atomic coordinates of the crystal structure of BuChE with bound butyrate (PDB code 1p0i) were used. All molecules of water were removed, along with other heteroatoms, to leave only the bound butyrate and the enzyme itself. Residues 1−3, 378−379, and 455, all of which were missing in the original crystal structure, were added using Swiss PDB Viewer v3.7. The added residues were briefly minimized within MOE (Chemical Computing Group, Montreal, Canada) using a sequence of SD, CG, and Truncated Newton algorithms; the AMBER99 force field and atom charges were used to model the protein throughout. Each inhibitor was rehybridized to sp^3 at the carbonyl carbon. The fragments distal to the carbamate were energy minimized using the MM94s force field.[37,38] The carbonyl oxygen was assigned a formal charge of −1. Inhibitor molecules were manually superim-

posed onto the butyrate fragment in the appropriate orientation, as carried out by Luo et al. in AChE.[34] The butyrate fragment was deleted and the inhibitor molecule covalently joined to O-χ of the active site serine, forming the desired intermediate. To prepare the complex for minimization, partial atomic charges for the nonstandard ligand atoms were calculated using MOPAC 7 (AM1-BCC method)[39] interfaced to MOE in a simplified system with the oxyanion hole residues removed. Because the total charge calculated for the inhibitor atoms was not an integer due to charge transfer between the inhibitor and Ser-198 during the reaction, the charge was altered on O-χ of the serine to give an overall charge of -1 on the inhibitor and Ser-198 atoms. AMBER 99 charges were calculated for the remaining protein atoms. The system was optimized for hydrogen bonding and protonation states for each residue in the protein were assigned using PDB2PQR[40] and Propka;[41] it was always ensured that Glu-325 and His-438 were appropriately protonated, such that the important hydrogen-bonding network of the catalytic triad was maintained. Subsequently, the whole system was energy minimized in MOE using sequential SD (100 steps) and TN (1000 steps or to an rms gradient of <0.01 kcal/(mol·A)) algorithms. The distances between the negatively charged carbonyl oxygen and the backbone nitrogens of the oxyanion hole residues were constrained, along with the distances between the hydrogen-bonding atoms of the catalytic triad. Generalized Born solvation was used with an interior dielectric constant of 20 and an exterior dielectric of 80. A nonbonded cutoff was applied, with a smoothing function applied between 12 and 15 Å. A second iteration of charge calculation and energy minimization was performed in an identical manner to arrive at the final models of the protein−carbamate adducts shown.

The interaction energies of the enzyme−ligand complexes were calculated using MOE. The interaction energies reported are the pairwise atomic interaction energies between the atoms of the ligand and all other atoms in the system. A reaction field model was used to describe electrostatic interactions, while all other parameters described for the minimization procedure were maintained when calculating these energies.

For the covalent docking procedure, the protein−ligand adduct was set up using Michel Sanner's Autodock Tools version 1.4.6, (http://autodock.scripps.edu/resources/adt), the graphical user interface to Autodock. The tetrahedral ligand of **2i** that had been produced using the procedures described above was extracted from the complex and set up for docking; eight rotable bonds were set in the ligand. The O-χ of serine in the adduct was changed to a covalent-binding atom type. The structure of *hu*BuChE with butyrate described above was used once again for docking, but in this case, the butyrate fragment was removed to leave only the protein itself. The protein was modified by deleting the side chain oxygen from Ser-198. Atomic affinity maps, an electrostatic potential map, and a covalent affinity map were computed using AutoGrid 3. The covalent affinity map was calculated using a spherically symmetric inverted Gaussian-shaped potential energy with a half-width of 5.0 Å and an energy penalty of 1000.0 kcal·mol^{-1}, with the minimum energy value centered on the coordinates of the χ-oxygen atom. In subsequent dockings, the covalently binding atom type in the adduct sought out this position, effectively binding the ligand to the protein. Autodock 3 was used to perform 50 independent dockings using the Lamarckian genetic algorithm, each starting from random initial positions. A population size of 300 was used for the search, with a maximum of 2.5 million energy evaluations. The results of these dockings were clustered using an rmsd tolerance of 3.0 Å. The highest scoring results were taken as indicative of the most appropriate binding mode for the ligand.

Acknowledgment. This work was supported by Science Foundation Ireland (05/RFP/CHE0046), Enterprise Ireland (BRGS2002), and IRCSET (Ciaran Carolan). We are grateful to Schwarz-Pharma, Shannon, Co. Clare for a gift of ISMN.

Supporting Information Available: Characterization data for compounds **1a**, **1b**, **1c**, **1e**, **1g**, **1i**, **1j**, **1k**, **21**, **2b**, **2c**, **2f**, **2g**, **2h**, **2k**, **2m**, **2n**, **2o**, **2p**, **2q**, **2s**, **4**; elemental analysis data, purity data by HPLC. This material is available free of charge via the Internet at http://pubs.acs.org.

References

(1) Francis, P. T.; Palmer, A. M.; Snape, M.; Wilcock, G. K. The cholinergic hypothesis of Alzheimer's disease: a review of progress. *J. Neurol. Neurosurg. Psychiatry* **1999**, *66*, 137–147.

(2) Bartus, R. T.; Dean, R. L.; Beer, B.; Lippa, A. S. The cholinergic hypothesis of geriatric memory dysfunction. *Science* **1982**, *217*, 408–417.

(3) Drachman, D. A.; Leavitt, J. Human memory and the cholinergic system. *Arch. Neurol.* **1974**, *30*, 113–121.

(4) Muñoz-Ruiz, P.; Rubio, L.; García-Palomero, E.; Dorronsoro, I.; del Monte-Millán, M.; Valenzuela, R.; Usán, P.; de Austria, C.; Bartolini, M.; risano, V.; Bidon-Chanal, A.; Orozco, M.; Luque, F. J.; Medina, M.; Martínez, A. Design, synthesis, and biological evaluation of dual binding site acetylcholinesterase inhibitors: new disease-modifying agents for Alzheimer's disease. *J. Med. Chem.* **2005**, *48*, 7223–7233.

(5) Bolognesi, M. L.; Cavalli, A.; Valgimigli, L.; Bartolini, M.; Rosini, M.; risano, V.; Recanatini, M.; Melchiorre, C. Multi-target-directed drug design strategy: from a dual binding site acetylcholinesterase inhibitor to a trifunctional compound against Alzheimer's disease. *J. Med. Chem.* **2007**, *50*, 6446–6449.

(6) Camps, P.; Formosa, X.; Muñoz-Torrero, D.; Petrignet, J.; Badia, A.; Clos, M. V. Synthesis and pharmacological evaluation of huprine−tacrine heterodimers: subnanomolar dual binding site acetylcholinesterase inhibitors. *J. Med. Chem.* **2005**, *48*, 1701–1704.

(7) Elsinghorst, P. W.; Cieslik, J. S.; Mohr, K.; Tränkle, C.; Gütschow, M. First gallamine−tacrine hybrid: design and characterization at cholinesterases and the M2 muscarinic receptor. *J. Med. Chem.* **2007**, *50*, 5685–5695.

(8) Brühlmann, C.; Ooms, F.; Carrupt, P. A.; Testa, B.; Catto, M.; Leonetti, F.; Altomare, C.; Carotti, A. Coumarins derivatives as dual inhibitors of acetylcholinesterase and monoamine oxidase. *J. Med. Chem.* **2001**, *44*, 3195–3198.

(9) Rodríguez-Franco, M. I.; Fernández-Bachiller, M. I.; Pérez, C.; Hernández-Ledesma, B.; Bartolomé, B. Novel tacrine−melatonin hybrids as dual-acting drugs for Alzheimer disease, with improved acetylcholinesterase inhibitory and antioxidant properties. *J. Med. Chem.* **2006**, *49*, 459–462.

(10) Fang, L.; Appenroth, D.; Decker, M.; Kiehntopf, M.; Roegler, C.; Deufel, T.; Fleck, C.; Peng, S.; Zhang, Y.; Lehmann, J. Synthesis and biological evaluation of NO-donor-tacrine hybrids as hepatoprotective anti-Alzheimer drug candidates. *J. Med. Chem.* **2008**, *51*, 713–716.

(11) Iwasaki, T.; Yoneda, M.; Nakajima, A.; Terauchi, Y. Serum butyrylcholinesterase is strongly associated with adiposity, the serum lipid profile and insulin resistance. *Intern. Med.* **2007**, *46*, 1633–1639.

(12) Mesulam, M. M.; Guillozet, A.; Shaw, P.; Levey, A.; Duysen, E. G.; Lockridge, O. Acetylcholinesterase knockouts establish central cholinergic pathways and can use butyrylcholinesterase to hydrolyze acetylcholine. *Neuroscience* **2002**, *110*, 627–639.

(13) Perry, E. K.; Perry, R. H.; Blessed, G.; Tomlinson, B. E. Changes in brain cholinesterases in senile dementia of Alzheimer type. *Neuropathol. Appl. Neurobiol.* **1978**, *4*, 273–277.

(14) Guillozet, A. L.; Smiley, J. F.; Mash, D. C.; Mesulam, M. M. Butyrylcholinesterase in the life cycle of amyloid plaques. *Ann. Neurol.* **1997**, *42*, 909–918.

(15) Greig, N. H.; Utsuki, T.; Ingram, D. K.; Wang, Y.; Pepeu, G.; Scali, C.; Yu, Q. S.; Mamczarz, J.; Holloway, H. W.; Giordano, T.; Chen, D.; Furukawa, K.; Sambamurti, K.; Brossi, A.; Lahiri, D. K. Selective butyrylcholinesterase inhibition elevates brain acetylcholine, augments learning, and lowers Alzheimer beta-amyloid peptide in rodent. *Proc. Natl. Acad. Sci. U.S.A.* **2005**, *102*, 17213–17218.

(16) Gilmer, J. F.; Moriarty, L. M.; McCafferty, D. F.; Clancy, J. M. Synthesis, hydrolysis kinetics and antiplatelet effects of isosorbide mononitrate derivatives of aspirin. *Eur. J. Pharm. Sci* **2001**, *14*, 221–227.

(17) Gilmer, J. F.; Moriarty, L. M.; Lally, M. N.; Clancy, J. M. Isosorbide-based aspirin prodrugs. II. Hydrolysis kinetics of isosorbide diaspirinate. *Eur. J. Pharm. Sci.* **2002**, *16*, 297–304.

(18) Gilmer, J. F.; Lally, M. N.; Gardiner, P.; Dillon, G.; Gaynor, J. M.; Reidy, S. Novel isosorbide-based substrates for human butyrylcholinesterase. *Chem. Biol. Interact.* **2005**, *157−158*, 317–319.

(19) Ellman, G. L.; Courtney, K. D.; Andres, V.; Featherstone, R. M. A New and Rapid Colorimetric Determination of Acetylcholinesterase Activity. *Biochem. Pharmacol.* **1961**, *7*, 88–95.

(20) Groner, E.; Ashani, Y.; Schorer-Apelbaum, D.; Sterling, J.; Herzig, Y.; Weinstock, M. The kinetics of inhibition of human acetylcholinesterase and butyrylcholinesterase by two series of novel carbamates. *Mol. Pharmacol.* **2007**, *71*, 1610–1617.

(21) Bartolucci, C.; Siotto, M.; Ghidini, E.; Amari, G.; Bolzoni, P. T.; Racchi, M.; Villetti, G.; Delcanale, M.; Lamba, D. Structural determinants of *Torpedo californica* acetylcholinesterase inhibition by the novel and orally active carbamate based anti-Alzheimer drug ganstigmine (CHF-2819). *J. Med. Chem.* **2006**, *49*, 5051−5058.

(22) Luo, W.; Yu, Q. S.; Zhan, M.; Parrish, D.; Deschamps, J. R.; Kulkarni, S. S.; Holloway, H. W.; Alley, G. M.; Lahiri, D. K.; Brossi, A. Novel anticholinesterases based on the molecular skeletons of furobenzofuran and methanobenzodioxepine. *J. Med. Chem.* **2005**, *48*, 986−994.

(23) Yu, Q.; Holloway, H. W.; Utsuki, T.; Brossi, A.; Greig, N. H. Synthesis of Novel Phenserine-Based-Selective Inhibitors of Butyrylcholinesterase for Alzheimer's Disease. *J. Med. Chem.* **1999**, *42*, 1855−1861.

(24) Saxena, A.; Redman, A. M.; Jiang, X.; Lockridge, O.; Doctor, B. P. Differences in active site gorge dimensions of cholinesterases revealed by binding of inhibitors to human butyrylcholinesterase. *Biochemistry* **1997**, *36*, 14642–14651.

(25) Carolan, C. G.; Gaynor, J. M.; Dillon, G. P.; Khan, D.; Ryder, S.; Reidy, S. A.; Gilmer, J. F. Novel isosorbide di-ester compounds as inhibitors of acetylcholinesterase. *Chem−Biol. Interact.* **2008**, 18606399. [Epub ahead of print], PMID.

(26) Li, B.; Sedlacek, M.; Manoharan, I.; Boopathy, R.; Duysen, E. G.; Masson, P.; Lockridge, O. Butyrylcholinesterase, paraoxonase, and albumin esterase, but not carboxylesterase, are present in human plasma. *Biochem. Pharmacol.* **2005**, *70*, 1673–1684.

(27) Khan, D.; Gilmer, J. F.; Carolan, C. G.; Gaynor, J. M.; Ryder, S. A. Pharmacological effects of a novel isosorbide-based butyrylcholinesterase inhibitor. *Chem.−Biol. Interact.* **2008**, 18606399. [Epub ahead of print] PMID.

(28) Harel, M.; Kleywegt, G. J.; Ravelli, R. B.; Silman, I.; Sussman, J. L. Crystal structure of an acetylcholinesterase−fasciculin complex: interaction of a three-fingered toxin from snake venom with its target. *Structure* **1995**, *3*, 1355–1366.

(29) Harel, M.; Quinn, D. M.; Nair, H. K.; Silman, I.; Sussman, J. L. The X-ray Structure of a Transition State Analog Complex Reveals the Molecular Origins of the Catalytic Power and Substrate Specificity of Acetylcholinesterase. *J. Am. Chem. Soc.* **1996**, *118*, 2340−2346.

(30) Harel, M.; Schalk, I.; Ehret-Sabatier, L.; Bouet, F.; Goeldner, M.; Hirth, C.; Axelsen, P. H.; Silman, I.; Sussman, J. L. Quaternary ligand binding to aromatic residues in the active-site gorge of acetylcholinesterase. *Proc. Natl. Acad. Sci. U.S.A.* **1993**, *90*, 9031–9035.

(31) Sussman, J. L.; Harel, M.; Frolow, F.; Oefner, C.; Goldman, A.; Toker, L.; Silman, I. Atomic structure of acetylcholinesterase from *Torpedo californica*: a prototypic acetylcholine-binding protein. *Science* **1991**, *253*, 872–879.

(32) Nicolet, Y.; Lockridge, O.; Masson, P.; Fontecilla-Camps, J. C.; Nachon, F. Crystal structure of human butyrylcholinesterase and of its complexes with substrate and products. *J. Biol. Chem.* **2003**, *278*, 41141–41147.

(33) Gao, D.; Zhan, C. G. Modeling effects of oxyanion hole on the ester hydrolysis catalyzed by human cholinesterases. *J. Phys. Chem. B* **2005**, *109*, 23070–23076.

(34) Luo, W.; Yu, Q. S.; Kulkarni, S. S.; Parrish, D. A.; Holloway, H. W.; Tweedie, D.; Shafferman, A.; Lahiri, D. K.; Brossi, A.; Greig, N. H. Inhibition of human acetyl- and butyrylcholinesterase by novel carbamates of (−)- and (+)-tetrahydrofurobenzofuran and methanobenzodioxepine. *J. Med. Chem.* **2006**, *49*, 2174–2185.

(35) Bar-On, P. M. C.; Harel, M.; Dvir, H.; Enz, A.; Sussman, J. L.; Silman, I. Kinetic and structural studies on the interaction of cholinesterases with the anti-Alzheimer drug rivastigmine. *Biochemistry* **2002**, *41*, 3555–3564.

(36) Morris, G. M.; Goodsell, D. S.; Halliday, R. S.; Huey, R.; Hart, W. E.; Belew, R. K.; Olson, A. J. Automated docking using a Lamarckian genetic algorithm and an empirical binding free energy function. *J. Comput. Chem.* **1998**, *19*, 1639–1662.

(37) Halgren, T. A. Merck molecular force field 0.1. Basis, form, scope, parameterization, and performance of MMFF94. *J. Comput. Chem.* **1996**, *17*, 490–519.

(38) Halgren, T. A. MMFF VII. Characterization of MMFF94, MMFF94s, and other widely available force fields for conformational energies and for intermolecular-interaction energies and geometries. *J. Comput. Chem.* **1999**, *20*, 730–748.

(39) Jakalian, A.; Bush, B. L.; Jack, D. B.; Bayly, C. I. Fast, efficient generation of high-quality atomic charges. AM1-BCC model: I. Method. *J. Comput. Chem.* **2000**, *21*, 132–146.

(40) Dolinsky, T. J.; Nielsen, J. E.; McCammon, J. A.; Baker, N. A. PDB2PQR: an automated pipeline for the setup of Poisson−Boltzmann electrostatics calculations. *Nucleic Acids Res.* **2004**, *32*, W665−W667.

(41) Li, H.; Roberston, A.; Jensen, J. H. Very fast empirical prediction and interpretation of protein pK_a values. *Proteins* **2005**, *61*, 704–721.

JM800564Y